Accuo - Needle Integrated Ultrasound Imaging

Project 11 Final Report, EN.600.446

Ernest Scalabrin
Mentors: Younsu Kim, H. Kai Zhang

Abstract

Lumbar punctures (LP) are used to acquire cerebrospinal fluid (CSF) for diagnostic and therapeutic purposes. 400,000 LPs are conducted annually in the U.S. and in some prevalent patient populations, the failure rate is over 50%. Accuo is a ultrasound embedded needle shaped probe meant to guide a physician to the subarachnoid space during a lumbar puncture procedure. The system we improved upon consists of a single disc shaped PZT element mounted to the tip of a 14G lumbar puncture introducer needle. The system creates a B-mode image by pulsing the element while sweeping it through tissue and tracking its angular position. Realtime scan conversion and beamforming algorithms were created in matlab. The beamformed imaging algorithm uses a technique known as backprojection which allows for a detailed image to be constructed from a single, unfocused beam swept over the field of interest. The techniques were optimized and analyzed for types of windowing functions, sizes of windows, and types of media. This technical progress will be continued by an undergraduate team over the summer of 2017 and through the next year.

Problem and Significance

LPs are performed to collect cerebrospinal fluid (CSF), an important bodily fluid needed to diagnose a variety of central nervous system disorders or conditions, especially life threatening ones like meningitis and encephalitis where a delay of a few hours can be catastrophic. The current standard of care utilizes anatomical landmarks to locate the L3-L5 intervertebral space, into which the lumbar puncture needle is inserted and advanced through many tissue layers to collect CSF in the subarachnoid space without hitting any nerves, blood vessels, or bone . Most lumbar punctures are performed blindly without the assistance of imaging or guidance mechanisms. Given this protocol, physicians can only accurately palpate the appropriate space about 30% of the time and perform a successful procedure after an average of 3 attempts. Blind entries can cause multiple failed punctures and the result in iatrogenic complications, including post-dural puncture headache, CSF leak, hematoma, and nerve damage.

Failed lumbar punctures can also subject patients to expensive, dangerous treatments. A common complication is a bloody tap occurring in 15% of patients, in which blood is present in the CSF sample. The presence of blood in CSF is typically seen in subarachnoid hemorrhage from rupture of an aneurysm and patients must undergo a cerebral angiogram to determine the source of bleeding. It is difficult to distinguish if blood in the CSF is due to a traumatic or bloody tap vs. true blood in the CSF from aneurysmal rupture. If physicians could avoid hitting blood vessels on the path to CSF, expensive and complex downstream procedures can be avoided. In addition, failed LP cases for patients with suspected meningitis result in prescription of broad-spectrum empiric antibiotics that increase the chance of antibiotic resistant bacteria in addition to a medically unnecessary admission to the hospital further driving up healthcare costs. An expensive fluoroscopic procedure must also be scheduled the following day, resulting in diagnostic delays and costly follow-up procedures. This is a common narrative for a variety of deep needle placement procedures, which would increase Accuo’s impact across medical disciplines.

Technology and Approach

Apparatus

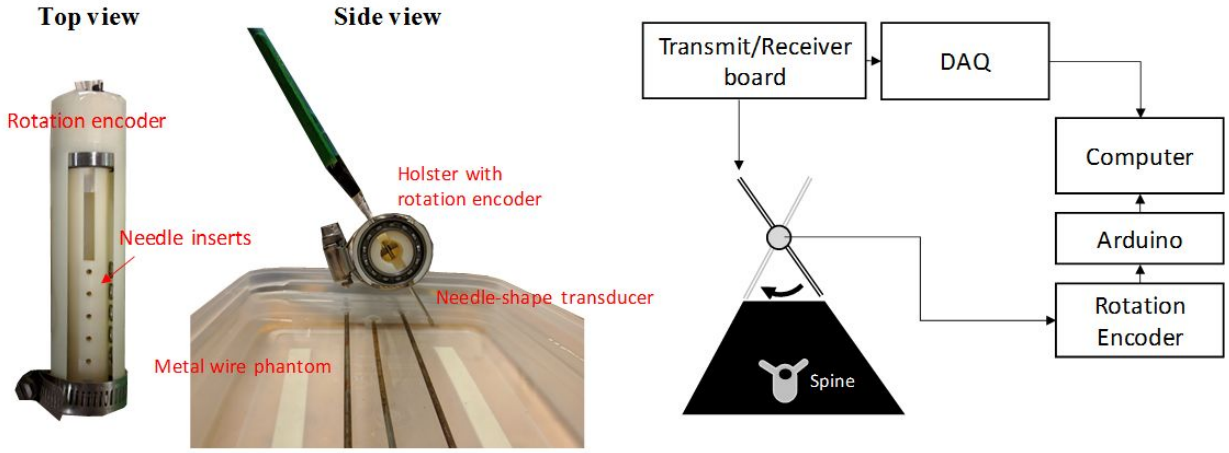

The apparatus consists of a needle shaped transducer with a 1mm PZT element fixed to the end, a rotational encoder, and the software necessary to construct a B-mode image. The needle is passed through the rotational encoder and swept across the field of interest. As the needle is being swept, the PZT is pulsed and individual A-line signals paired with their respective angle data are collected. The software then uses this data to construct a 2D B-mode image. In a clinical setting, the encoder would be fixed to a patient's back, and as the needle is slowly being inserted into the outer adipose tissue, the physician would sweep the needle over the target of interest. The system would provide dynamic, 2D image guidance without significantly altering the flow of the procedure.

Realtime Simulation

In a clinical scenario, individual A-line data would be passed from the device to the software. This data would then be paired with its corresponding angular value with respect to the patient. In order to simulate this data acquisition, previously collected A-line data is passed into our algorithm individually and in the order that they were collected. This allowed for more streamlined testing of our algorithms and the avoidance of wasting resources for each test.

Backprojection

A transducer with a single small PZT element has a very wide signal distribution in space. This translates to poor spatial resolution because features which are not in the path of the element will contribute to A-line readings. However, using backprojection based synthetic aperture focusing, this lack of spatial resolution can be attenuated by accentuating the differences between adjacent A-line in a given window.

As angular offset from the line normal to the element increases, the intensity of the signal decreases and as a result, A-lines which are more offset from the signal carry less weight. One way to accomplish this efficiently is to use a windowing function (or apodization function). An apodization function is simply a function which is equal to zero outside a given interval. In order to mimic the dropoff of signal intensity as described above, the functions used in this algorithm are smooth bell shaped curves.

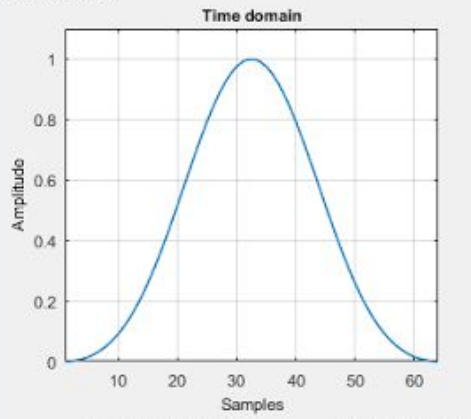

Blackman

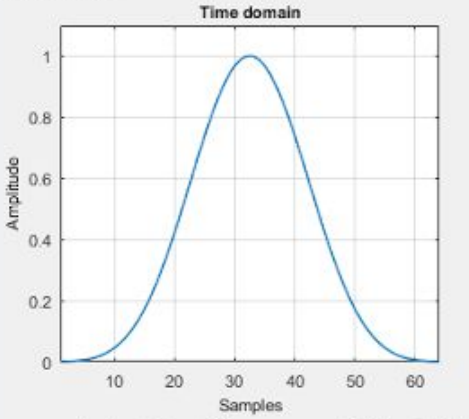

Chebyshev

Hann

Kaiser

For a given A-line signal, an arbitrary window size is chosen, then this A-line is multiplied by a chosen windowing function and added to its adjacent A-lines (which may be empty or not collected yet). In order to avoid decreased signal on the sides of the image due to less neighboring A-lines compared to the center, a count of the number of iterations of backprojection is kept and the data is divided by this count. Even though data at the center will have more contributing neighbors it will be reduced by a count variable which is proportional to this contribution. As a result, image brightness is kept constant.

```
for l = 1:numberOfLines %reading A-lines one by one
    beamformedData(:, l) = rawData(:, l);
    %iterate through window for this a line
    for w = l - ((windowSize-1)/2): l + ((windowSize-1)/2)
        %make sure adjacent a line is valid
        if w > 0 && w <= numberOfLines
           width = depthOfNeedle*sind(abs(l-w)*angleDist);
            %iterate down a line
            for s = 1:samplesPerLine
                    beamformedData(s, w) = beamformedData(s, w) + apodWindow(w - l + (windowSize - 1)/2 + 1)*rawData(s, l);
                    count(s, w) = count(s, w) + 1;
            end
        end

    end
    beamformedData = beamformedData./count;
```

The above figure is an example of the matlab code used to accomplish backprojection of A-line data. In order to further demonstrate this concept, a single A-line was passed through the algorithm and the output is seen below. The window size is large to demonstrate the concept.

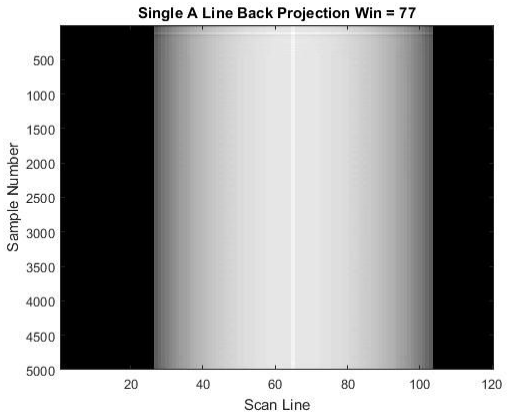

Scan Conversion

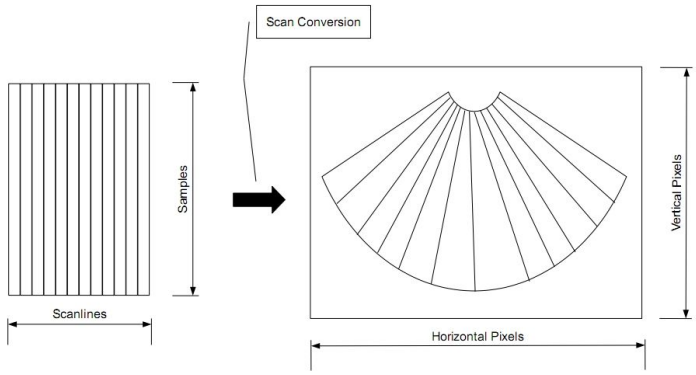

After the data has been backprojected, the data must be scan converted. Scan conversion (SC) is simply the conversion of data from polar coordinates to cartesian coordinates. In the case of this device, the angular data paired with a particular A-line is used to calculate its position in the cartesian plane.

```
%% Scan Conversion stuff %%
%NEEDS CHANGE

for W = 1 - ((windowSize-1)/2): 1 + ((windowSize-1)/2) %iterate through backprojection window

    if W > 0 && W <= size(beamformedData, 2)
    currentALine = (beamformedData(:, W));
    currentALine = convn(currentALine, Filt.BPF', 'same');
    currentAngle = middleAngle - dataAngleSet(W);%middle angle - current angle or angle from midline (left is positive, right is negative)
        for j = 500:samplesPerLine
        %horizontal calculations
        distanceFromProbe = sampleSpacing*j; %straight line distance from probe
        xDistanceFromMiddle = (distanceFromProbe+depthOfNeedle)*sind(currentAngle); %horizontal distance of sample from midline
        xCoordinate = round((xSize/2) - xDistanceFromMiddle);
        %vertical calculations
        yCoordinate = round(100*((depthOfNeedle + distanceFromProbe)*cosd(currentAngle)));
        cartesianMatrix(yCoordinate - 2500, xCoordinate+100) = currentALine(j);
        end
    end
end
```

The above figure is an example of the matlab code used to accomplish scan conversion. The output of this simple algorithm after the removal of noisy interface data from the first 500 samples is seen below.

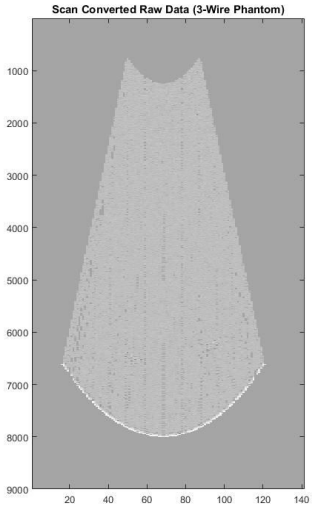

Analysis

In order to determine the most effective window size and windowing function for our apparatus and application, the full width at half maximum across the peak intensity of the output of a point source input to our algorithm was measured.

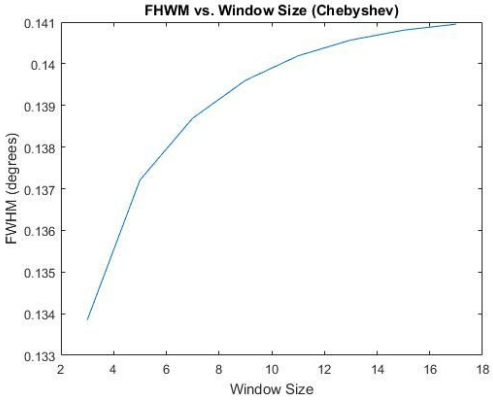

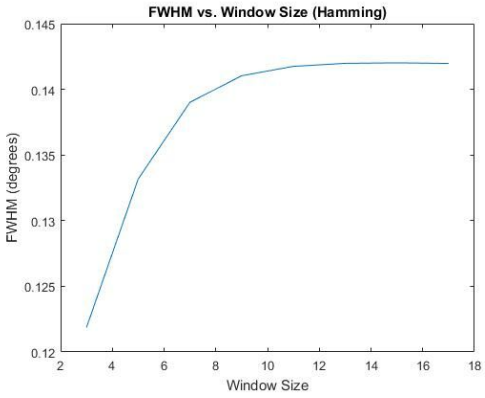

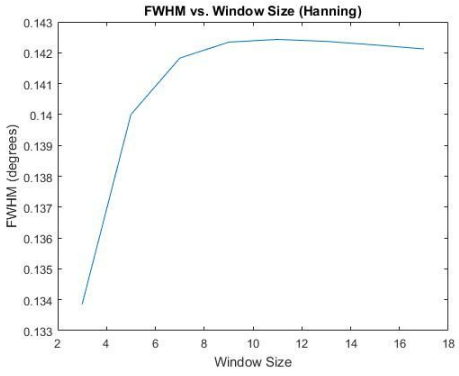

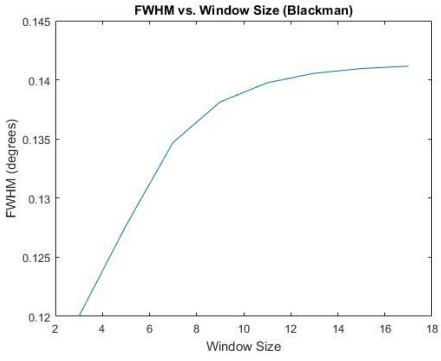

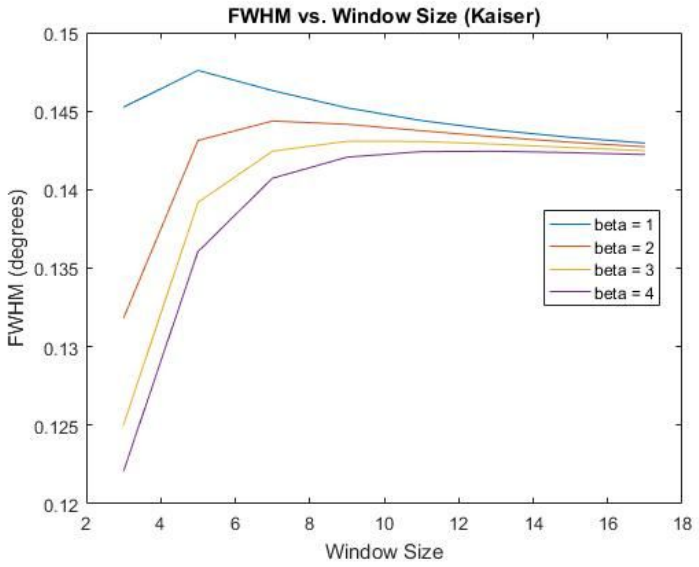

In addition to FWHM analysis, comparison of the noise level in the output output of real data from a wire phantom and ex-vivo tissue while varying window size was also conducted. (see figure below)

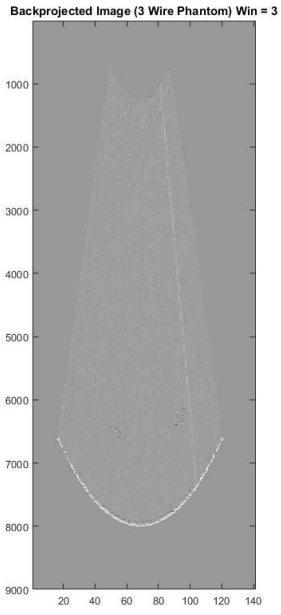

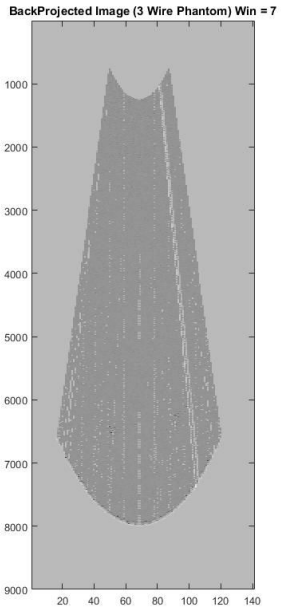

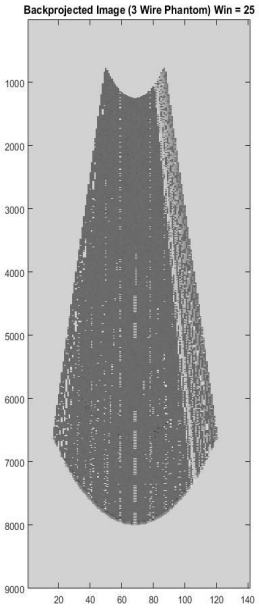

Results/Discussion

As seen in the figures above, most of the functions FWHM plateau at a window size of between 8 and 12. This indicates that no more useful information can be derived from having a window size of greater than 12. Qualitatively, it appears that window size and noise levels are inversely related. As seen in the figures above, the wires can be visualized at win = 3, but due to noise are no longer visible at win = 7 let alone win = 25. Comparing the results below across media and target types it is clear that this method has potential for backprojection in realtime.

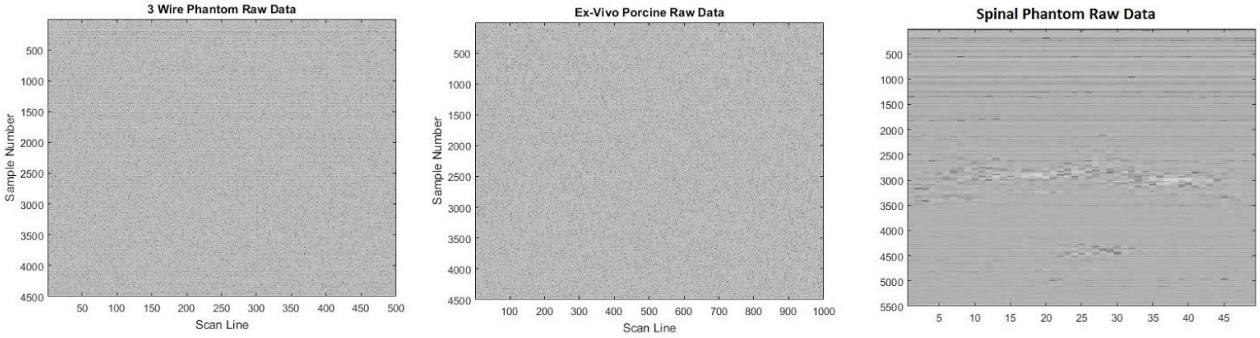

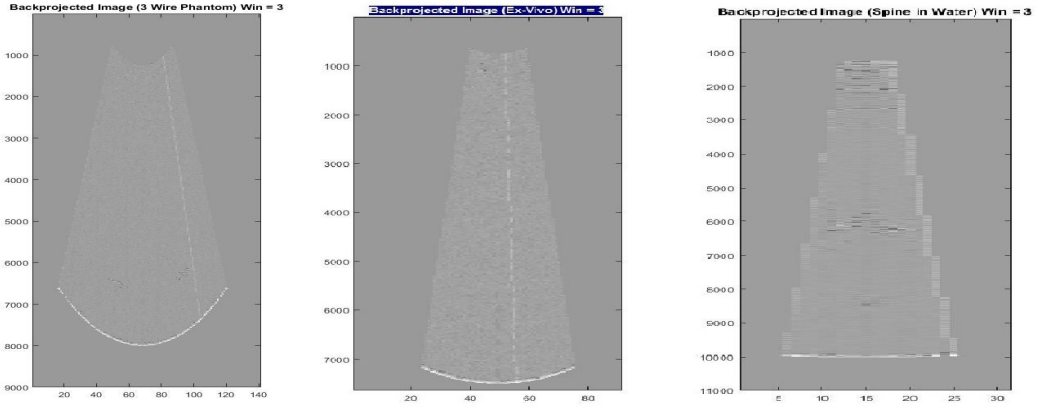

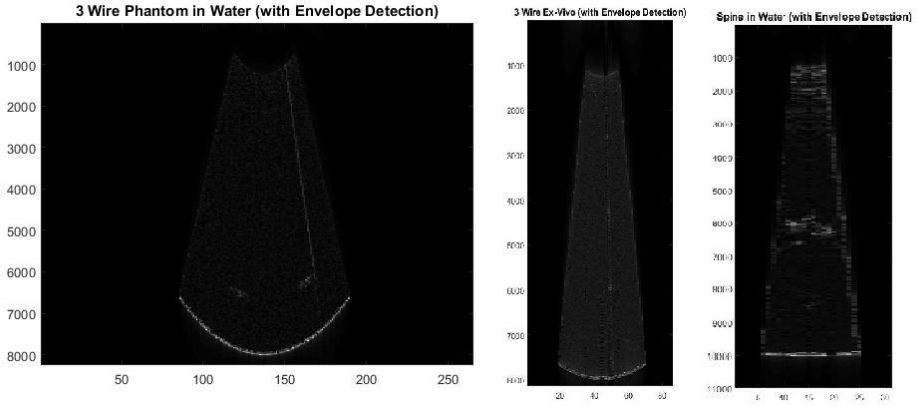

Management Summary

This project experienced significant setbacks throughout the semester as a result of technical malfunction of our Windows 10 and 7 PC's. I spent too much time trying to get the realtime code working on the machines instead of simulating realtime data acquisition. This set us back significantly and as a result our actual progress was very different from our projected progress. The initial and current goals and milestones are seen below. In addition, because of a lack of access to a computer which was able to run the DLLs necessary for the realtime data acquisition and processing, our adjusted maximum deliverable was not met. I will be passing off the code to 2 other members of the undergraduate team to work on during this summer.

Estimated Dates of Task Completion:

1. ~~C++ integration (In parallel with below code)~~
2. Beamforming and Scan Conversion
    a. Understand the Code (3/1/17)
        i. Beamforming (2/27/17)
        ii. Scan Conversion (3/1/17)
    b. Able to implement Existing algorithm (3/6/17)
    c. Study Literature (3/13/17)
    d. Add real time scan conversion visualization in matlab (3/17/17)
    e. Backprojection reconstruction (3/24/17)
3. ~~Depth Tracking~~
    ~~a. Take images of wire phantom (3/31/17)~~
    ~~b. Attempt to use cross correlation to discern depth (4/6/17)~~
    ~~c. Fabricate needle with side shooting element (4/13/17)~~
        ~~i. Or mechanical tracking (4/20/17)~~
        ~~ii. Or optical tracking (4/20/17)~~
    ~~d. Integrate side shooting signal into algorithm (4/30/17)~~

Actual Dates of Task Completion

1. Simulated Realtime Scan Conversion Matlab Algorithm (4/12/17)
2. Simulated Realtime Beamforming Matlab Algorithm (5/15/17)
3. Realtime Integration of Algorithms (Not Completed)

References

[1] Armon C., Evans R. W., "Addendum to assessment: prevention of post-lumbar puncture headaches," Neurology 65, 510-512 (2005).
[2] American Society for Healthcare Risk Management, "Risk Management Handbook for Health Care Organizations", Jossey-Bass, 5 (2009).
[3] Edwards C., Leira E. C., and Gonzalez-Alegre P., "Residency Training: A Failed Lumbar Puncture Is More about Obesity than Lack of Ability," Neurology 84(10), e69-72 (2015).
[4] Shah K. H., Richard K. M., et al., "Incidence of traumatic lumbar puncture," Academic Emergency Medicine 10(2), 151-4 (2003).
[5] Ahmed S. V., Jayawarna C., and Jude E., "Post lumbar puncture headache: Diagnosis and management," Postgraduate Medical Journal 82(273), 713-716 (2006).
[6] Shaikh F., Brzezinski J., Alexander S., Arzola C., Carvalho J. C., Beyene J., and Sung L., "Ultrasound imaging for lumbar punctures and epidural catheterisations: systematic review and meta-analysis," BMJ 346 (2013).
[7] Brook A. D., Burns J., Dauer E., Schoendfeld A. H., and Miller T. S., "Comparison of CT and Fluoroscopic Guidance for Lumbar Puncture in an Obese Population with Prior Failed Unguided Attempt," Journal of NeuroInterventional Surgery 323-27 (2013).
[8] Engedal T. S., Ørding H., Vilholm O. J., "Changing the needle for lumbar punctures," Clinical Neurology and Neurosurgery 130, 74-79 (2015).
[9] Tamas U., Abolmaesumi P., Jalal R., Welch M., Ayukawa I., Nagpal S., Lasso A., Jaeger M., Borschneck D., Fichtinger G., and Mousavi P., "Spinal Needle Navigation by Tracked Ultrasound Snapshots," IEEE Transactions on Biomedical Engineering 59(10), 2766-72 (2012).
[10]Moore J., Clarke C., Bainbridge D., Wedlake C., Wiles A., Pace D., and Peters T., "Image Guidance for Spinal Facet Injections Using Tracked Ultrasound," Medical Image Computing and Computer-Assisted Intervention, (2009).
[11]Chen E. C. S., Mousavi P., Gill S., Fichtinger G., Abolmaesumi P., "Ultrasound guided spine needle insertion," Proc. SPIE 7625, 762538 (2010).
[12]Najafi M., Abolmaesumi P., Rohling R., "Single-Camera Closed-Form Real-Time Needle Tracking for UltrasoundGuided Needle Insertion," Ultrasound in Medicine and Biology, 41(10), 2663-2676 (2015).
[13]Wang X. L., Stolka P. J., Boctor E., Hager G., Choti M., "The Kinect as an interventional tracking system," Proc. SPIE 8316, 83160U (2012).
[14]Nagpal S., Abolmaesumi P., Rasoulian A., et al., "A multi-vertebrae CT to US registration of the lumbar spine in clinical data," Int. J. CARS 10(9), 1371-81 (2015).
[15]Jensen J. A., Nikolov S. I., Gammelmark K. L., Pedersen M. H., "Synthetic aperture ultrasound imaging," Ultrasonics 44(22), e5-e15 (2006).
[16]Zhang H. K., Cheng A., Bottenus N., Guo X., Trahey G. E., Boctor E. M., "Synthetic Tracked Aperture Ultrasound (STRATUS) Imaging: Design, Simulation, and Experimental Evaluation," Journal of Medical Imaging 3(2), 027001 (2016).
[17]Bottenus N., Long W., Zhang H. K., Jakovljevic M., Bradway D. P., Boctor E. M., Trahey G. E., "Feasibility of Swept Synthetic Aperture Ultrasound Imaging," IEEE Transactions on Medical Imaging 35(7), 1676-1685 (2016).